Pharm Res (2013) 30:1883–1895
DOI 10.1007/s11095-013-1031-6

RESEARCH PAPER

Improving Intracellular Doxorubicin Delivery Through Nanoliposomes Equipped with Selective Tumor Cell Membrane Permeabilizing Short-Chain Sphingolipids

Lília R. Cordeiro Pedrosa • Albert van Hell • Regine Süss • Wim J. van Blitterswijk • Ann L. B. Seynhaeve • Wiggert A. van Cappellen • Alexander M. M. Eggermont • Timo L. M. ten Hagen • Marcel Verheij • Gerben A. Koning

Received: 1 December 2012 / Accepted: 12 March 2013 / Published online: 11 May 2013

ABSTRACT

Purpose To improve nanoliposomal-doxorubicin (DoxNL) delivery in tumor cells using liposome membrane-incorporated short-chain sphingolipids (SCS) with selective membrane-permeabilizing properties. DoxNL bilayers contained synthetic short-chain derivatives of known membrane microdomain-forming sphingolipids; C_8-glucosylceramide (C_8-GluCer), C_8-galactosylceramide (C_8-GalCer) or C_8-lactosylceramide (C_8-LacCer).

Methods DoxNL enriched with C_8-GluCer or C_8-GalCer were developed, optimized and characterized with regard to size, stability and drug retention. *In vitro* cytotoxic activity was studied in a panel of human tumor cell lines and normal cells. Intracellular Dox delivery was measured by flow cytometry and visualized by fluorescence microscopy. For a further understanding of the involved drug delivery mechanism confocal microscopy studies addressed the cellular fate of the nanoliposomes, the SCS and Dox in living cells.

Results C_8-LacCer-DoxNL aggregated upon Dox loading. In tumor cell lines SCS-DoxNL with C_8-GluCer or C_8-GalCer demonstrated strongly increased Dox delivery and cytotoxicity compared to standard DoxNL. Surprisingly, this effect was much less pronounced in normal cells. Nanoliposomes were not internalized, SCS however transfered from the nanoliposomal bilayer to the cell membrane and preceded cellular uptake and subsequent nuclear localization of Dox.

Conclusion C_8-GluCer or C_8-GalCer incorporated in DoxNL selectively improved intracellular drug delivery upon transfer to tumor cell membranes by local enhancement of cell membrane permeability.

Electronic supplementary material The online version of this article (doi:10.1007/s11095-013-1031-6) contains supplementary material, which is available to authorized users.

L. R. C. Pedrosa • A. L. B. Seynhaeve • A. M. M. Eggermont • T. L. M. ten Hagen
Laboratory Experimental Surgical Oncology
Section Surgical Oncology, Department of Surgery
Erasmus Medical Center,
PO Box 2040, Rotterdam 3000 CA, The Netherlands

G. A. Koning (✉)
Laboratory Experimental Surgical Oncology
Section Surgical Oncology, Department of Surgery
Erasmus Medical Center, Room Ee151b
PO Box 2040, Rotterdam 3000 CA, The Netherlands
e-mail: g.koning@erasmusmc.nl

A. van Hell • M. Verheij
Division of Biological Stress Response
The Netherlands Cancer Institute - Antoni van Leeuwenhoek Hospital,
Plesmanlaan 121 Amsterdam 1066 CX, The Netherlands

R. Süss
Department of Pharmaceutical Technology and Biopharmacy
Albert-Ludwigs University, Freiburg 79104 Germany

W. J. van Blitterswijk
Division of Cellular Biochemistry, The Netherlands Cancer Institute - Antoni van Leeuwenhoek Hospital, Plesmanlaan 121
Amsterdam 1066 CX, The Netherlands

W. A. van Cappellen
Optical Imaging Centre, Erasmus Medical Center,
PO Box 2040, Rotterdam 3000 CA, The Netherlands

A. M. M. Eggermont
Institut de Cancerologie Gustave Roussy, Villejuif Paris 94800, France

M. Verheij
Department of Radiotherapy The Netherlands Cancer Institute - Antoni van Leeuwenhoek Hospital,
Plesmanlaan 121 Amsterdam 1066 CX, The Netherlands

KEY WORDS doxorubicin-nanoliposome · short chain sphingolipid · Tumor cell membrane permeabilization

ABBREVIATIONS

C_8-GluCer	C_8-glucosylceramide
C_8-GalCer	C_8-galactosylceramide
C_8-LacCer	C_8-lactosylceramide
D:PL ratio	Drug to phospholipid initial mass ratio
Dox	Doxorubicin
FCS	Fetal calf serum
HSPC	Hydrogenated soy phosphatidylcholine
DSPE-PEG_{2000}	1,2-distearoyl-sn-glycero-3-phosphoethanolamine-N-PEG_{2000}
MIF	Mean of fluorescence intensity
NBD PE	1,2-dipalmitoyl-*sn*-glycero-3-phosphoethanolamine-N-(7-nitro-2-1,3-benzoxadiazol-4-yl)
NL	Nanoliposomes
pdi	Polydispersity index
SCS	Short chain sphingolipids
SEM	Standard error of the mean
TCMM	Tumor cell membrane modulation

INTRODUCTION

Insufficient uptake of chemotherapeutic agents by tumor cells remains an important limitation in clinical cancer treatment. Several factors play a role such as suboptimal dosing due to systemic toxicity, rapid drug clearance from circulation and limited drug traversal across the tumor cell membrane. Here we addressed these hurdles using advanced drug delivery technologies. Liposomes, small nanovesicles composed of phospholipids, cholesterol and poly(ethylene glycol) (PEG)-lipids, are used to entrap the chemotherapeutic agent prolonging systemic drug concentrations and reducing dose-limiting toxicities (1). In addition, nanoliposomes (NL), due to their small size (< 100 nm), can accumulate in tumor tissue by virtue of the enhanced permeability and retention effect (EPR) (2–5). In this study nanoliposomal delivery is combined with a novel strategy using short-chain sphingolipids (SCS) to enhance transmembrane drug transport (6–8).

Sphingolipids are key molecules for assembly of microdomains in the cell membrane, (9–11). Evidence exists that SCS self-association may lead to domain or channel formation in the membrane (12) and may explain the enhanced passage of amphiphilic drugs across cell membranes (6). In this study we exploited this property of SCS to develop pegylated-nanoliposomal doxorubicin (DoxNL) formulations.

Dox is a chemotherapeutic agent whose mode of action includes intercalation between adjacent base pairs of the DNA double helix, binding to DNA-associated enzymes such as topoisomerase, and effects on membranes (13,14). DoxNL (Caelyx®/Doxil®) increased drug accumulation in solid tumors and reduced dose-limiting toxicities such as myelosuppression and cardiotoxicity (15–17). DoxNL is currently approved for use in AIDS-related Kaposi's sarcoma (18), refractory ovarian cancer (19), myeloma (20) and metastatic breast cancer (16,18,21). Although DoxNL, due to its favorable pharmacokinetic profile and small size, accumulates in tumors, its ability to deliver the Dox content to its active site intracellularly (bioavailability) remains a main issue. DoxNL is characterized by high stability to prevent drug release in circulation, causing slow and suboptimal drug delivery to tumor cells upon accumulation in the tumor area (22,23). The inadequate Dox release together with its slow intracellular uptake likely are main reasons for the limited efficacy increase of DoxNL in cancer patients (16,18,24). In order to improve intracellular Dox delivery we combined nanoliposomal drug delivery with the concept of tumor cell membrane modulation (TCMM) using SCS.

Regarding the mechanism of enhanced drug delivery from SCS enriched nanoliposomes we hypothesize that they transfer spontaneously from the NL bilayer to cell membranes creating enhanced cellular accessibility for amphiphilic compounds by the formation of specific domains with increased drug permeability or transient pores which improve drug influx. The aim of this study is to further optimize and explore SCS-based nanoliposomal drug delivery using various synthetic SCS and investigate the involved drug delivery mechanism.

MATERIALS AND METHODS

Materials

Hydrogenated soy phosphatidylcholine (HSPC) and distearylphosphatidylethanolamine (DSPE)-PEG_{2000} were from Lipoid (Ludwigshaven, Germany). Short chain sphingolipids, C_8-glucosylceramide (C_8-GluCer), C_8-galactosylceramide (C_8-GalCer), C_8-lactosylceramide (C_8-LacCer) and fluorescent lipid NBD PE (1,2-dipalmitoyl-*sn*-glycero-3-phosphoethanolamine-N-(7-nitro-2-1,3-benzoxadiazol-4-yl) (ammonium salt) and C_6-NBD Galactosyl Ceramide N-[6-[(7-nitro-2-1,3-benzoxadiazol-4-yl)amino]hexanoyl]-D-galactosyl-ß1-1'-sphingosine were from Avanti Polar Lipids (Alabaster, AL, USA).

Polycarbonate filters were from Northern Lipids (Vancouver, BC, Canada) and PD-10 Sephadex columns were from GE Healthcare (Diegem, Belgium). Dox-HCl (Dox) was from Pharmachemie (Haarlem, The Netherlands). Cholesterol, HEPES (2-[4-(2-hydroxyethyl)piperazin-1-yl] ethanesulfonic acid), trichloroacetic acid (TCA), acetic acid, Triton-X, sulforhodamine B (SRB) were from Sigma Aldrich (Zwijndrecht, The Netherlands). Hoechst was from Molecular Probes (Leiden, The Netherlands). PBS was from Boom and FACS flow fluid from BD Biosciences.

Preparation of SCS-NL

Nanoliposomes were formulated of HSPC/Cholesterol/DSPE-PEG_{2000} in a molar ratio of 1.85: 1: 0.15. Liposomes of 85–100 nm in diameter were prepared by lipid film hydration and extrusion at 65°C. Drug loading was based on ammonium sulfate gradient method (25). To the mixture of lipids, 0.05, 0.1 or 0.15 mol of SCS was added per mole of total amount of lipid (including cholesterol) and liposomes were formulated as described previously (8). Dox was added to liposomes in different drug to phospholipid ratios (w/w) - 0.25:1, 0.2:1, 0.15:1 and 0.1:1 for 1 h at 65°C. Non encapsulated Dox was separated by ultracentrifugation at 29000 rpm in a Beckman ultracentrifuge (Ti50.2 rotor). The liposome pellet was resuspended in buffer containing 135 mM NaCl, 10 mM HEPES, pH 7.4.

Size and polydispersity index (pdi) were determined by light scattering using a Zetasizer Nano ZS (Malvern Instruments, Malvern, UK). Lipid concentration was measured by phosphate assay (26).

NBD PE was incorporated in the formulation at 0.25 mol% of total lipid as a stable fluorescent bilayer marker. Studies assessing the fate of liposomal SCS used a similar mol% of bilayer incorporated C_6-NBD-Galactosyl Ceramide.

Loading Efficiency

After separation of free non-encapsulated Dox from nanoliposomal encapsulated Dox, the amount of entrapped Dox was measured by fluorimetry ($\lambda_{Exitation}$ 475 nm; $\lambda_{Emission}$ 590 nm). Total amount of drug was measured after entire liposome solubilization with 1% (v/v) Triton in water to a sample from stock liposomal Dox.

Stability

Long-term storage conditions stability (4°C) was based on size, pdi and Dox content measurements for a period of at least 6 months. All measurements were performed in triplicate. Dox content was measured by fluorimetry ($\lambda_{Exitation}$ 475 nm; $\lambda_{Emission}$ 590 nm), after separation of free/entrapped drug by gel filtration chromatography. Stability at 37°C, in the presence and absence of serum was studied for a period of 24 h by fluorimetry. Total drug release was measured after entire liposomal solubilization by adding 1% (v/v) of Triton-X. The percentage of drug content was calculated following the formula:

$$\frac{100 - \left(\text{Flourescence}_{\text{sample}} - \text{blank}\right)}{\text{Flourescence}_{\text{total release}} - \text{blank}} \times 100$$

Cryo-transmission Electron Microscopy (TEM)

Cryo-TEM was used to characterize the detailed structure of the liposomal formulations (non-enriched, 10 mol% C_8-GluCer and 10 mol% C_8-GalCer-NL) of Dox and the physical state of the encapsulated drug, as previously described (27,28). The freezing was performed in a cooling chamber, which was permanently cooled with liquid nitrogen. A sample droplet was placed on a microperforated copper grid and blotted by a filter paper to result in a thin liquid film. The grid was plunged into liquid ethane for immediate freezing. A Leo 912 Omega TEM microscope (Carl Zeiss NTS GmbH, Oberkochen, Germany) was used.

Cell Culture

In vitro anti-tumor activity was studied towards a panel of human tumor cell lines: BLM and Mel57 melanomas, MCF7 and SKBR3 breast carcinoma and ASPC1 and Panc1 pancreatic carcinomas. All tumor cell lines were cultured in Dulbeccos's modified Eagle medium, supplemented with 10% fetal calf serum and 4 mM L-glutamine. HUVEC were isolated by collagenase digestion using the method described by Jaffe *et al.* (29) and cultured in HUVEC medium containing human endothelial serum free medium (Invitrogen), 20% heat inactivated newborn calf serum (Cambrex), 10% heat inactivated human serum (Cambrex), 20 ng/ml human recombinant epidermal basic fibroblast growth factor (Peprotech EC Ltd), 100 ng/ml human recombinant epidermal growth factor (Peprotech EC Ltd) in fibronectin (Roche Diagnostics) coated flasks. Fibroblasts (3T3) were purchased from Biowhitakker and cultured in Dulbeccos's modified Eagle medium containing nutrient mixture F12, supplemented with 10% fetal calf serum and 4 mM L-glutamine.

Cells were subcultured weekly by trypsinization when a confluency of 80–90% was achieved and maintained in a water saturated atmosphere of 5% CO_2 at 37°C.

Cell Toxicity

All cell lines were plated in flat bottom 96 well-plates. Tumor cells were seeded at cell densities obtained from respective tumor growth curves to ensure use of cells in their log-phase of growth. BLM and Mel57 melanoma cells were seeded at a density of 3×10^3 and 6×10^3 cells/well, respectively. 1.25×10^4 cells/well were used for breast carcinoma cells MCF7 and SKBR3. For ASPC1 and Panc1 pancreatic carcinoma cell lines 6×10^3cells/well were seeded. HUVEC and 3T3 fibroblast cells were seeded at a density of 1×10^4 cells/well and 5×10^3cells/well, respectively, in order to achieve the same confluency.

After 24 h, cells were exposed to serial concentrations of Dox-liposomal formulations (SCS enriched and non-enriched) in culture medium for 24 h.

Cell survival was determined by measuring total cellular protein levels using the sulforhodamine-B (SRB) assay (30). Cells were washed twice with PBS, incubated with 10% trichloric acetic acid (1 h, 4°C) and washed again. Cells were stained with 0.4% SRB (Sigma) for 15 min, washed with 1% acetic acid. After drying, protein-bound SRB was dissolved in TRIS buffer (10 mM, pH 9.4) and absorbance was measured at a wavelength of 540 nm in a plate reader. Cell survival was calculated as a percentage relative to control (untreated cells), which was set at 100%.

IC_{50} was determinate for each Dox liposomal formulation, by plotting the cell survival observed for each concentration *versus* the log of the concentration and fitting a non linear regression curve using GraphPad Prism software v5.0. All experiments were performed in triplicates and were repeated at least 3 times, independently.

Cell survival quantification was complemented by evaluation of cellular morphology. Following the same cellular concentration from SRB assay, BLM, Mel57, MCF7, SKBR3, Panc1 and ASPC1 cells were plated in a 24 well plate and allow to growing for 24 h. The cells were treated with Dox (1 μM, 10 μM or 100 μM) in its non-enriched and enriched (C_8-GluCer and C_8-GalCer) liposomal form. After 24 h cell morphology was examined with a 10× N.A 0.30 Plan Neofluar objective lens using an inverted Zeiss Axiovert 100M microscope equipped with an Axiocam digital camera (Carl Zeiss).

Intracellular Drug Uptake by Flow Cytometry

Intracellular Dox levels in BLM, MCF7 and ASPC1 cells were measured by flow cytometry. Cells were seeded on flat bottom 24 well plates at a final concentration of 6×10^4 cells/well and incubated for 24 h. Non-enriched and SCS enriched-DoxNL, with C_8-GluCer or C_8-GalCer, diluted in growth medium were added in a drug concentration of 1 μM and 10 μM, after which cells were incubated for 1, 4 and 24 h. After incubation, cells were washed twice to discard non-incorporated drug and trypsinized for 2 min. Cell suspensions were washed twice in medium and resuspended in PBS. Cellular uptake was measured on a Becton Dickinson FACScan using Cell Quest software. Excitation was set at 488 nm and detection by FL2 detector channel.

Intracellular Drug Uptake by Fluorescence Microscopy

MCF7, BLM and ASPC1 cells in a concentration of 1×10^5 cells/well were seeded on a cover glass coated with 0.1% collagen and incubated for 24 h. Hoechst (1:100) was added for 20 min cells and washed twice before adding 10 μM of Dox in form of non enriched-DoxNL or SCS-enriched DoxNL. Cells were incubated at 37°C for 1 and 4 h and using fluorescence microscopy intracellular drug uptake was evaluated in living cells, using a filter set consisting of a 450–490 nm band pass excitation filter for Hoechst and a 510 nm beam splitter and a 520–543 nm long pass excitation filter for Dox. Cells were imaged using a 40× oil immersion objective.

Intracellular Drug Uptake by Confocal Microscopy

BLM melanoma, MCF7 breast carcinoma and ASPC1 pancreatic carcinoma cells were cultured on a cover glass of 25 mm diameter coated with 0.1% collagen and incubated for 24 h in cultured medium. Cell density was 1×10^5 cells for BLM melanoma cells, MCF7 breast carcinoma and ASPC1 pancreatic carcinoma cells. Non-enriched liposomal Dox and SCS enriched liposomal Dox was added in a concentration of 10 μM. Cells were incubated for 4 h. Dox uptake was studied using a Zeiss LSM 510 META confocal microscope using 488 argon laser for NBD-PE (500–550 nm band pass filter), a 405 nm Diode laser for Hoechst (420–480 nm band pass filter) and a 543 nm Helium-Neon laser for Dox (560–615 nm band pass filter). Images of the different incubations were taken using identical settings for laser power and photomultipliers.

Intracellular Fate of SCS and Doxorubicin

Labelled NBD-C_6-GalCer-DoxNL was followed in time in BLM melanoma cells (1×10^5 cells) during treatment for 40 min. A Leica SP5 (Leica Mannheim) confocal microscope was used with 488 nm excitation and BP 500–550 nm emission of the SCS and 561 nm excitation and BP 570 nm–650 nm emission for Dox with a 63× plan apo (na 1.4) lens. Six optical planes were recorded with an interval of 1.22 μm and a pinhole at 1 airy unit.

Doxorubicin was giving by direct excitation with the 488 excitation line, a crosstalk in the SCS emission channel. The amount of crosstalk was measured (35%) and the SCS images were corrected for this crosstalk. To remove some photon noise from the images, a Gaussian filter was applied to the time lapse images with ImageJ (Rasband, W.S., ImageJ, U. S. National Institutes of Health, Bethesda, Maryland, USA, http://imagej.nih.gov/ij/, 1997–2011). To increase the weak SCS signal a contract stretch was performed.

Statistics

Statistical analysis was performed using the ANOVA test. P-values less than 0.05 were considered statistically significant.

All parametric values are expressed as mean ± standard error of the mean (SEM). Calculations were performed using GraphPad Prism v5.0.

RESULTS

Optimizing C_8-GluCer-DoxNL

C_8-GluCer-DoxNL with optimal density of the SCS at 10 mol% (8) were optimized with regard to drug loading. Formulations were loaded at Dox:PL ratios of 0.25:1, 0.2:1, 0.15:1 or 0.1:1 (w/w). The size of the final liposomes after loading was smaller than 100 nm and the pdi ≤ 0.1 and a loading efficiency > 90% was achieved at a Dox:PL ratio of 0.1:1 for both C_8-GluCer-DoxNL and DoxNL (Table I). To study the effect of Dox:PL ratio on *in vitro* anti-tumor efficacy, 10 mol% C_8-GluCer–DoxNL loaded with the different Dox:PL ratios were tested in human BLM melanoma (Fig. 1a) and human MCF7 breast carcinoma (Fig. 1b) cell lines. Treatment with 10 mol% C_8-GluCer–DoxNL for 24 h, decreased cell viability at increasing DoxNL concentration, but was not affected by different Dox:PL ratios in either cell line (Fig. 1 and Supplementary Material Table SI).

To assess C_8-GluCer-DoxNL stability, drug retention was studied during long-term storage at 4°C and under cell culture conditions at 37°C in the presence of 10% FCS. During long-term storage, C_8-GluCer-DoxNL had similar stability as DoxNL, showing a minor release of ≤ 10% Dox over 6 months (Table II). Also under culture conditions (37°C with 10%FCS), C_8-GluCer-DoxNL efficiently retained more than 90% of their contents (Table II and Supplementary Material Fig. S1), and was comparable to DoxNL.

Novel DoxNL Enriched with C_8-GalCer or C_8-LacCer

In addition to C_8-GluCer, two other short-chain C_8-glycosphingolipids, with galactosyl (C_8-GalCer) and lactosyl (C_8-LacCer) head groups, (Fig. 2) were evaluated as possible alternative SCS to enhance drug uptake from DoxNL. Formulations were characterized with regard to size, pdi, loading efficiency and stability. At a SCS density of 10 mol% and loaded with Dox at a 0.1:1 Dox:PL (w/w) ratio, C_8-GalCer-DoxNL presented ideal size (<100 nm) and pdi (<0.1), high loading efficiency and a long-lasting stability. At a higher Dox:PL ratio of 0.2:1, Dox loading of C_8-GalCer-DoxNL was still > 90%, but pdi increased to 0.16 (Table II). In contrast, C_8-LacCer-DoxNL could not be prepared successfully at either ratio as they strongly aggregated immediately upon Dox loading, resulting in large particle size, pdi and low drug loading efficiency.

Upon long-term storage at 4°C, C_8-GalCer-DoxNL had similar stability profile as C_8-GluCer-DoxNL and DoxNL, showing a minor release of ≤ 10% Dox over 6 months (Table II) and no changes in particle size or pdi. (Supplementary Material Table SII). Under culture conditions (37°C with 10%FCS) C_8-GalCer–DoxNL efficiently retained more than 90% of their contents (Table II and Supplementary Material Fig. S1), comparable to both C_8-GluCer-DoxNL and DoxNL.

Optimal C_8-GalCer Enriched DoxNL

C_8-GalCer-DoxNL was prepared at different SCS densities and at a Dox:PL initial mass ratio of 0.1:1. Densities of C_8-GalCer up to 15 mol% did not negatively affect size, pdi or drug loading of the DoxNL (Table III).

In vitro efficacy studies on MCF7 breast, human BLM melanoma and ASPC1 pancreatic carcinoma cells (Fig. 3 and Supplementary Material Table SIII) demonstrated that a density of 10 mol% resulted in the strongest anti-tumor activity in all cell lines. A higher density of 15 mol% did not further increase efficacy relative to 10 mol%.

Transmission Electron Microscopy of SCS-DoxNL

Non-enriched DoxNL and DoxNL enriched with C_8-GluCer or C_8-GalCer were analyzed by cryogenic Transmission Electron Microscopy (cryo-TEM) (Fig. 4). DoxNL were round shaped, uniform in size and most particles were characterized by an intraliposomal gel like precipitate of Dox. C_8-GluCer-DoxNL and C_8-GalCer-DoxNL, which had a

Table I Characterization of C_8-GluCer Enriched Liposomes Loaded at Different Drug to Phospholipid Mass Ratios

Drug:PL $(w/w)_i$	SCS-DoxNL	Size (nm) ± SEM	pdi ± SEM	% Load ± SEM
0.25:1	Non-enriched	109 ± 6.7	0.08 ± 0.01	79 ± 4.1
	10% C_8-GluCer	99 ± 5.7	0.08 ± 0.01	74 ± 4.6
0.2:1	Non-enriched	95 ± 4.9	0.1 ± 0.03	68 ± 10.2
	10% C_8-GluCer	98 ± 7.8	0.19 ± 0.04	69 ± 10.9
0.15:1	Non-enriched	89 ± 3.7	0.09 ± 0.01	92 ± 2.0
	10% C_8-GluCer	86 ± 2.4	0.09 ± 0.02	78 ± 8.2
0.1:1	Non-enriched	89 ± 2.0	0.07 ± 0.01	96 ± 5.7
	10% C_8-GluCer	84 ± 1.1	0.07 ± 0.01	91 ± 5.0

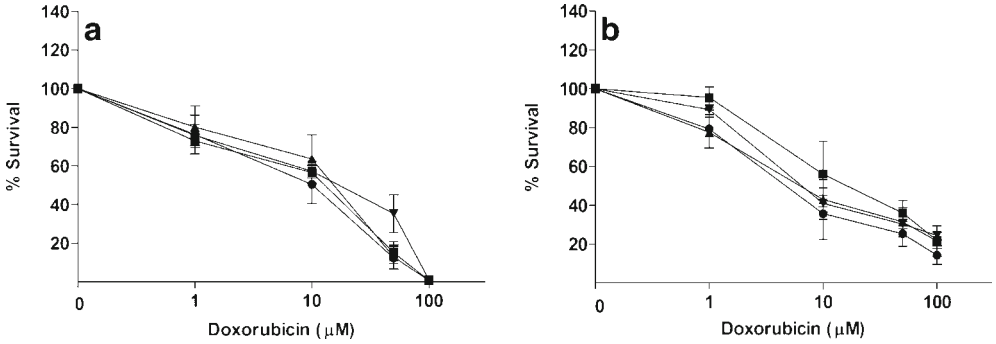

Fig. 1 *In vitro* efficacy study of C_8-GluCer-DoxNL loaded with doxorubicin at different Dox:PL ratios (w/w), 0.25: 1 (●), 0.2:1 (■), 0.15:1 (▲) and 0.1:1 (▼). Different Dox:PL loading ratios did not affect the efficacy of enriched C_8-GluCer-DoxNL in **a** BLM, melanoma and **b** MCF7 breast carcinoma cell line when incubated for 24 h at 37°C. Cell survival was analyzed by SRB assay and values represent the mean ± SEM, n ≥3.

normal round shape before Dox-loading (data not shown), were observed as round and rod-shaped vesicles after Dox-loading. Round vesicles were observed with and without Dox precipitate, rod-shaped particles all contained the typical Dox precipitate and had a width of approximately 40 nm and varied in length between 100 and 200 nm. In the C_8-GalCer-DoxNL formulation occasionally more elongated rod-like particles with a length of up to 500 nm were observed.

SCS-enriched-DoxNL exert selective cytotoxicity towards tumor cells

In vitro drug efficacy of the optimized SCS enriched DoxNL was tested in a panel of human tumor cell lines, including BLM and Mel57 melanoma, MCF7 and SKBR3, breast and Panc1 and ASPC1 pancreatic carcinoma, as well as in normal cells: endothelial cells (HUVEC) and 3T3 fibroblasts. In all tumor cell lines, C_8-GluCer-DoxNL and C_8-GalCer-DoxNL exerted increased cytotoxicity, compared to DoxNL during 24 h incubation. IC_{50} values of tumor cell treatments with both SCS-enriched formulations dropped significantly by 5 to 50-fold in comparison with DoxNL and commercially available Doxil®, $P<0.05$ (Table IV and Supplementary Material Fig. S2a). Despite the fact that SCS-enrichment of DoxNL increased toxicity towards Mel57 and Panc1 cell lines, the differences were somewhat less pronounced as compared to the other tumor cell lines. No major differences were observed between C_8-GluCer-DoxNL and C_8-GalCer-DoxNL efficacy towards the various tumor cell lines. Strikingly, cytotoxicity of SCS-DoxNL towards normal endothelial cells and fibroblasts was much less pronounced, with IC50 values that are either indifferent between SCS-DoxNL or DoxNL or show a slight drop of less than 2-fold. In HUVEC, C_8-GluCer-DoxNL showed a toxicity profile comparable to DoxNL and Doxil®. On the other hand, C_8-GalCer-DoxNL had a somewhat more pronounced toxicity towards HUVEC than C_8-GluCer-DoxNL at high drug concentrations. In turn, C_8-GluCer-DoxNL showed to be of equally low toxicity to fibroblasts as C_8-GalCer-DoxNL with comparable IC_{50} values. Empty SCS-NL were tested on MCF7 breast carcinoma cell line and no toxicity was caused by the presence of C_8-GluCer or C_8-GalCer in the liposomal bilayer (data not shown) at equimolar lipid concentrations to SCS-DoxNL.

In vitro drug efficacy was qualitatively confirmed by evaluating cellular morphology after treatment with free Dox, Doxil, non-enriched and SCS-enriched-DoxNL (Supplementary Material Fig. S2b). All other tested tumor cell lines showed similar results as the BLM melanoma cell line (data not shown).

Table II Characterization and Stability of Different Glycoceramide-Enriched Liposomes

Drug:PL (w/w)i	SCS-DoxNL	Size (nm) ± SEM	pdi ± SEM	%Load ± SEM	% Encapsulated Dox (after 6 months at 4°C) ± SEM	% Encapsulated Dox (after 15 h at 37°C) ± SEM
0.1:1	Non-enriched	89 ± 2.0	0.07 ± 0.01	96 ± 5.7	91 ± 4.4	91 ± 9.1
	10% C_8-GluCer	84 ± 1.1	0.07 ± 0.01	91 ± 5.0	88 ± 5.3	98 ± 1.9
	10% C_8-GalCer	92 ± 4.0	0.09 ± 0.02	96 ± 2.8	91 ± 3.3	100 ± 9.5
	10% C_8-LacCer	482 ± 36.2	0.47 ± 0.07	9 ± 2.9	nd *	nd
0.2:1	10% C_8-GalCer	93 ± 4.0	0.16 ± 0.05	98 ± 9.5	nd	nd
	10% C_8-LacCer	395 ± 29.0	0.58 ± 0.07	7 ± 2.9	nd	nd

* *nd* not determined

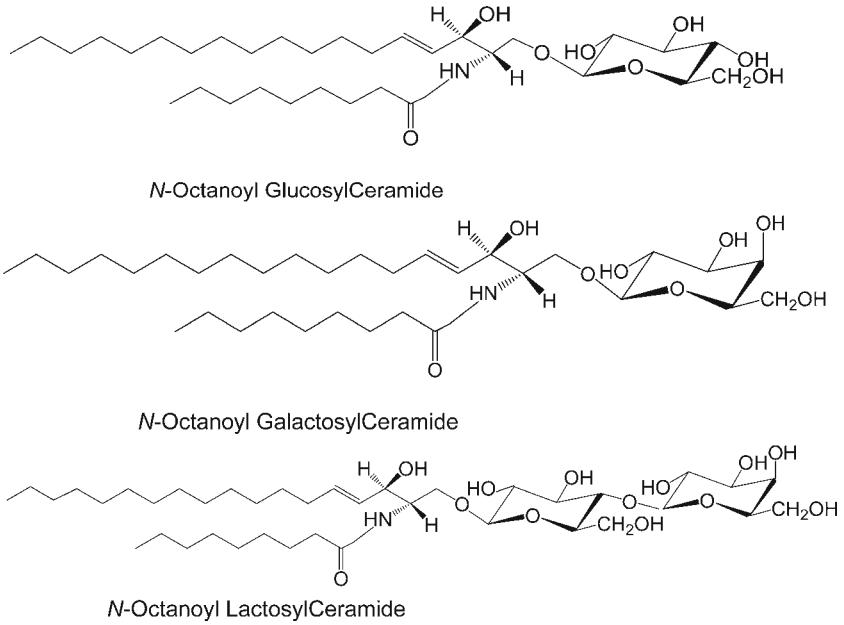

Fig. 2 Short chain sphingolipid molecular structures. C_8-GluCer and C_8-GalCer differ in the position of one hydroxyl group in the sugar moiety position, which is equatorial and axial, respectively. C_8-LacCer presents a more complex sugar moiety. Chem Draw v8.0 was used to draw molecular structures.

Quantification of SCS-enriched-DoxNL Potential as Drug Uptake Enhancers

The effect of SCS enrichment of DoxNL on intracellular Dox uptake was quantified by flow cytometry. BLM melanoma, MCF7 breast carcinoma and ASPC1 pancreatic carcinoma cell lines were treated with DoxNL, C_8-GluCer-DoxNL or C_8-GalCer-DoxNL at drug concentrations of 10 or 1 μM for 1, 4 or 24 h (Fig. 5a and Supplementary Material Fig. S4a, respectively). Intracellular drug uptake increased in time for both SCS-DoxNL formulations in all cell lines, whereas only minor drug uptake was observed in cells incubated with DoxNL for 24 h. At all drug concentrations and incubation times tested, SCS-DoxNL induced higher intracellular drug levels than DoxNL. Upon incubation with 10 μM SCS-DoxNL a high intracellular drug uptake was achieved after 4 h, with little to no increase in uptake upon prolonging the incubation to 24 h. This is caused by cytotoxicity effects affecting drug uptake measurements at 24 h. At a 10-fold lower concentration, which causes much less cytotoxicity during 24 h, drug levels continued to increase up to 24 h (Supplementary Material Fig. S4). Whereas C_8-GalCer after 4 h of incubation at 10 μM gives similar results in all three cell lines, C_8-GluCer seemed to increase Dox uptake in BLM cells (45.2 ± 1.2) to a higher extent than MCF7 (22.3 ± 5.9) and ASPC1 cells (24.4 ± 3.9) (Fig. 5b). A similar trend can be seen at 1 μM, where C_8-GluCer improves Dox delivery to BLM more strongly than C_8-GalCer (Supplementary Material Fig. S4b).

Fluorescence Microscopic Imaging of Intracellular Drug Delivery

Evaluation of intracellular drug uptake by life cell fluorescence microscopy (Fig. 6) supported the outcome of flow cytometry measurements. After 4 h of incubation, non-enriched DoxNL still did not show considerable intracellular drug delivery, whereas both SCS-enriched DoxNL established high intracellular Dox levels. Similar to the observations obtained by flow cytometry, BLM cells showed increased Dox uptake from C_8-GluCer-DoxNL compared to C_8-GalCer-DoxNL. Dox from SCS enriched-DoxNL showed faint cytoplasmic staining, and mainly accumulated in the nucleus as confirmed by a Hoechst co-staining.

Cellular Fate of SCS-NL and Doxorubicin

Confocal microscopy experiments were performed to further confirm the intracellular localization of Dox and nanoparticles. After 4 h incubation, both enriched DoxNL

Table III Optimal Density of C_8-GalCer-enriched Pegylated DoxNL

Drug:PL 0.1:1 (w/w)$_i$	Size (nm) ± SEM	pdi ± SEM	% Load ± SEM
0% C_8-GalCer-DoxNL	89 ± 2.0	0.07 ± 0.01	96 ± 5.7
5% C_8-GalCer-DoxNL	84 ± 1.2	0.06 ± 0.01	97 ± 4.3
10% C_8-GalCer-DoxNL	92 ± 4.0	0.09 ± 0.02	96 ± 2.8
15% C_8-GalCer-DoxNL	83 ± 3.2	0.06 ± 0.01	103 ± 1.1

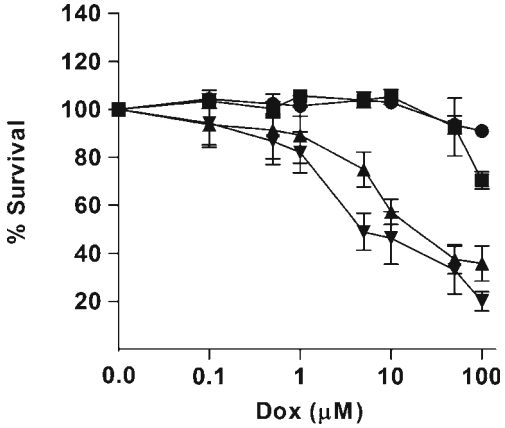

Fig. 3 *In vitro* efficacy study in MCF7, breast carcinoma cell line incubated with different density of C_8-GalCer in DoxNL, 0 mol% (●), 5 mol% (■), 10 mol% (▲) and 15 mol%(▼) in a Dox:PL mass ratio of 0.1:1. 15 mol % content of C_8-GalCer did not give additional cytotoxicity compared to 10 mol% content. Values represent the mean ± SEM (n≥3).

achieved high intracellular drug levels. Dox accumulated in the nucleus to a high extent, whereas also cytoplasmic Dox was observed. Liposome internalization was not observed by MCF7, breast carcinoma cells (Fig. 7), BLM melanoma or ASPC1 pancreatic carcinoma cell lines (Supplementary Material Fig. S3). The absence of tumor cell DoxNL internalization was evidenced by the lack of cell associated liposomal bilayer marker NBD-PE, which was found extracellularly surrounding the cells whereas at the same time Dox showed some cytoplasmic staining and high levels in the nucleus.

Intracellular Localization of SCS and Doxorubicin

Time-lapse confocal microscopy experiments were performed directly after starting the incubation of cells with SCS-enriched liposomes to further study the intracellular localization of Dox and SCS. Three-dimensional reconstructions of cellular stacks in time were used to create a movie representing cellular uptake of the SCS, Dox and their co-localization in time (Supplementary Material Movie 1).

In time, fluorescently labeled SCS were observed to transfer from the DoxNL bilayer to the cell membrane (Fig. 8 and Supplementary Material Movie 1). This transfer was observed already at 5 min after start of the incubation and preceded cellular Dox uptake, which was observed only at 10 min after adding liposomes to the cells. Doxorubicin entered the cell and prominently accumulated in the nucleus within the subsequent 30 min. In addition, appreciable Dox-levels were detected in the cytoplasm at 25–40 min (Fig. 8).

SCS transferred to the cell membrane were later also found intracellular in the cytoplasm, but were not associated with the nucleus or with its membrane.

DISCUSSION

The use of SCS-enriched nanoliposomes to improve drug-cell membrane traversal is a novel drug delivery concept and represents an advanced and versatile technology to enhance Dox delivery into tumor cells and thereby its efficacy as a chemotherapeutic drug. Previously, we were able to demonstrate that DoxNL enriched with C_8-GluCer strongly enhanced Dox delivery and subsequent anti-tumor efficacy both *in vitro* and *in vivo* (7,8). In the present study a further optimization and characterization of C_8-GluCer-DoxNL was performed, in terms of drug loading, liposome size, pdi, drug entrapment efficiency and morphology, all representing important criteria for translation of this formulation towards future clinical application. In addition, DoxNL with other synthetic short-chain glycosphingolipids were studied for drug uptake enhancement, of which C_8-

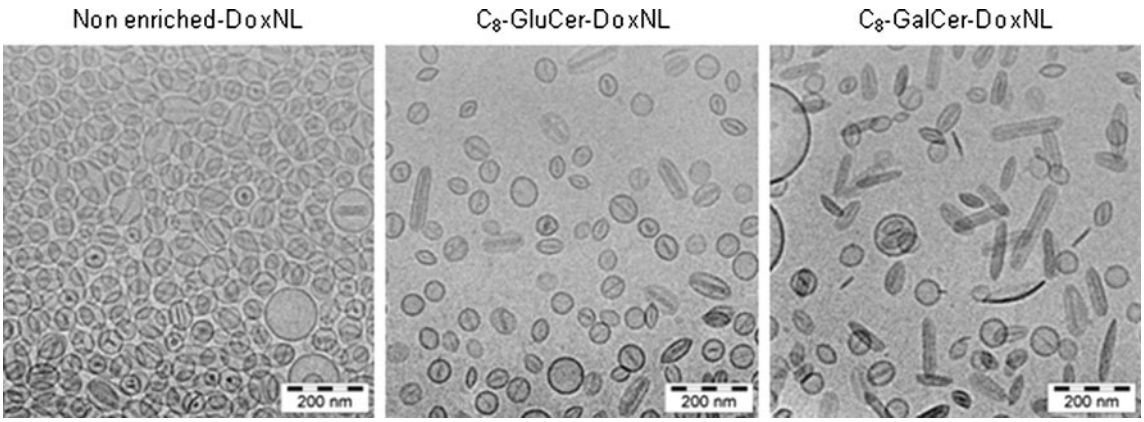

Fig. 4 Cryo-TEM images of HSPC/Chol/PEG liposomes with or without SCS, loaded with doxorubicin in a Dox:PL ratio of 0.1:1. A clear drug precipitate is visible inside liposomes. SCS-enriched DoxNL have more elongated rod-like structures upon loading with Dox. The bar in the micrograph represents 200 nm. A 12500× magnification was used.

Table IV *In Vitro* Cytotoxicity (IC_{50}, μM) of SCS-enriched-DoxNL and Standard Pegylated Liposomal Doxorubicin in Tumor and Non-tumor Cell Lines. At least three independent experiments were performed and values represent the mean ± SEM. * $P < 0.05$ *versus* DoxNL

	IC_{50} (μM)			
	Doxil	DoxNL	10% C_8-GluCer DoxNL	10% C_8-GalCer DoxNL
Tumor cells				
BLM	>150	>150	10.0 ± 2.2*	9.1 ± 0.4*
Mel57	>150	>150	31.0 ± 7.2*	34.1 ± 18.2*
MCF7	>150	>150	10.8 ± 2.3*	6.9 ± 2.0*
SKBR3	>150	>150	3.1 ± 0.9*	5.3 ± 4.5*
Panc1	>150	>150	29.2 ± 7.1*	25.4 ± 3.3*
ASPC	>150	>150	10.1 ± 1.6*	23.1 ± 17.3*
Non tumor cells				
HUVEC	>150	>150	>150	87.7 ± 7.1
3T3	>150	>150	101.7 ± 17.4	103.3 ± 8.6

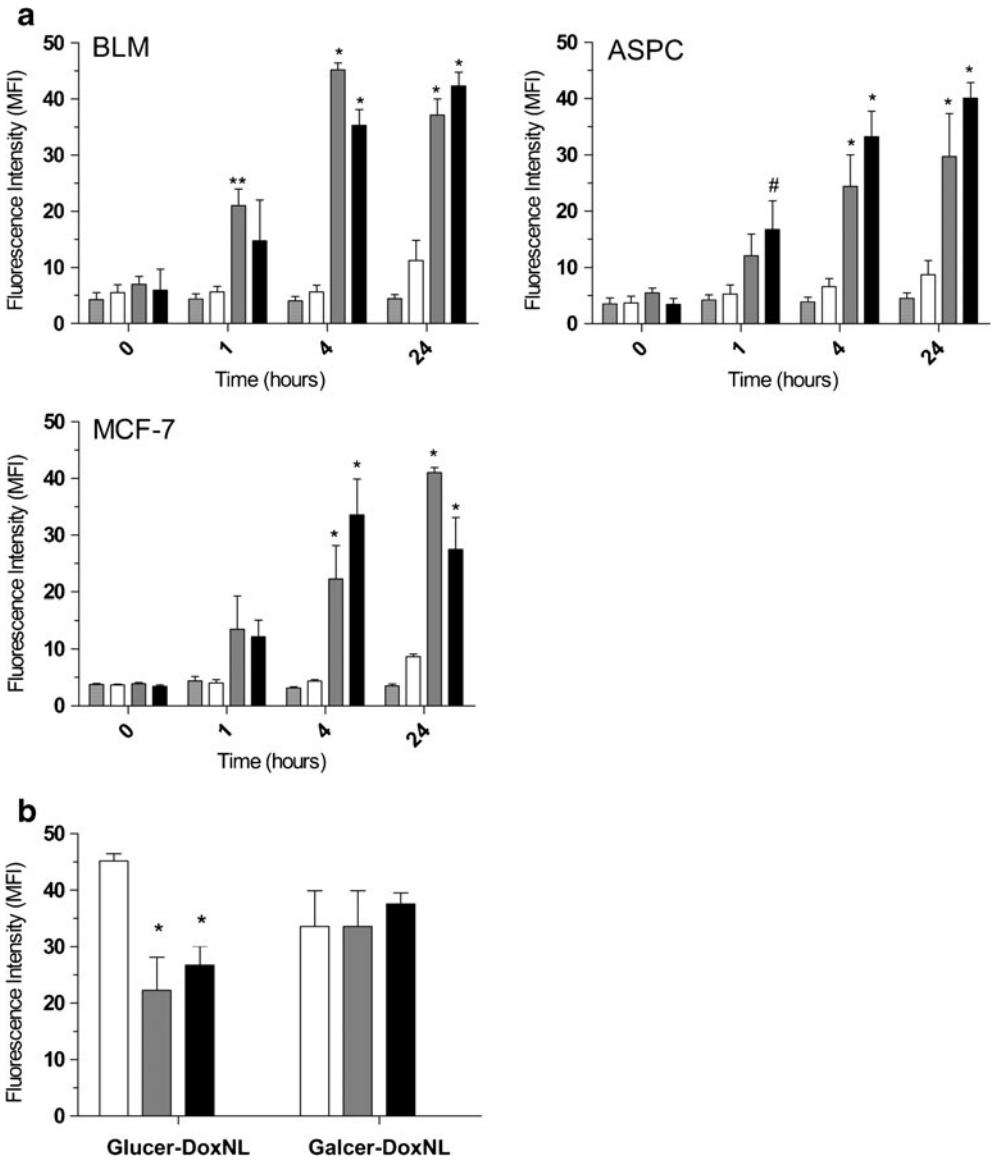

Fig. 5 Intracellular Dox uptake after treatment with DoxNL, 10 μM was quantified by flow cytometry in BLM melanoma, MCF7 breast carcinoma and ASPC1 pancreatic carcinoma (**a**). Doxorubicin was formulated in non enriched-DoxNL (open), 10% C_8-GluCer-DoxNL (*dark grey*) and 10% C_8-GalCer-DoxNL (*black*). Fluorescence of non treated cells was measured as a control (*bright grey*). At least three independent experiments were performed and values represent the mean ± SEM; *, $P < 0.001$; **, $P < 0.01$ and #, $P < 0.05$ *versus* non enriched-DoxNL at the same time point. (**b**) Overview of Dox uptake by 3 different tumor cell lines incubated with 10 μM C_8-GluCer or C_8-GalCer-DoxNL after 4 h of incubation. C_8-GalCer-DoxNL gave similar results in all three cell lines, C_8-GluCer seemed to increase Dox uptake in BLM (open) cells when compared to MCF7 (*grey*) and ASPC1 (*black*) cells.

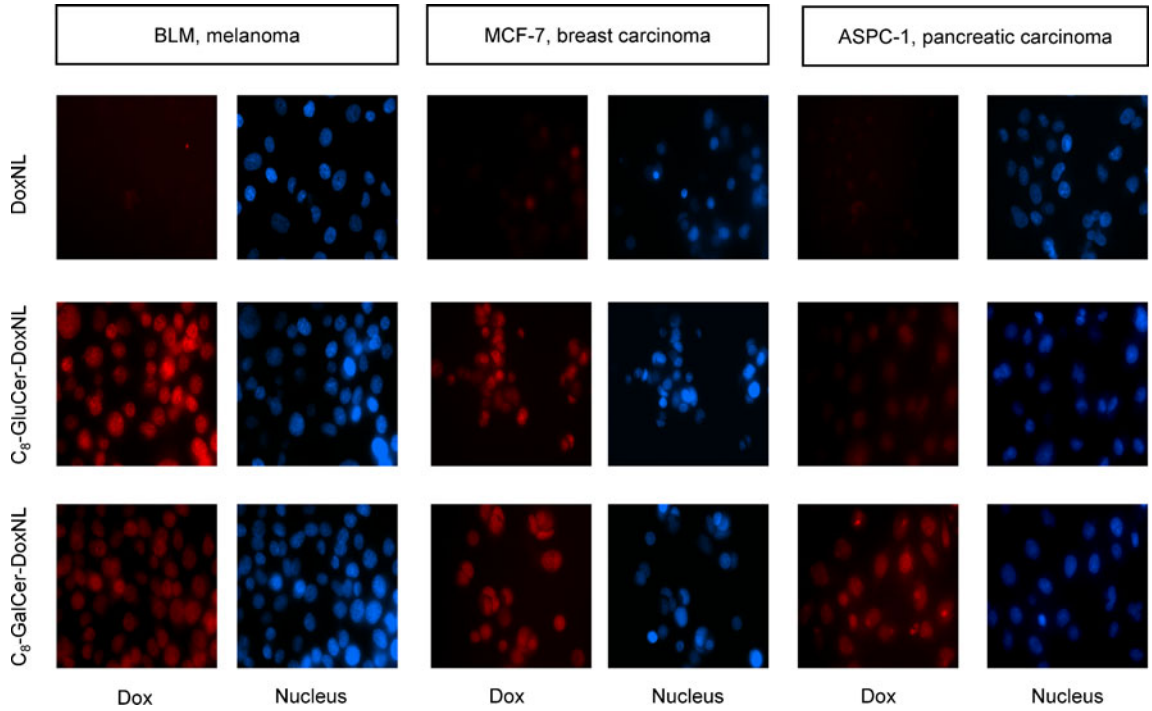

Fig. 6 Fluorescence microscopy images of BLM, melanoma cell line (**a**), MCF7 breast carcinoma cell line (**b**) and ASPC1, pancreatic carcinoma cell line (**c**), after 4 h of treatment with 10 μM of doxorubicin formulated in standard non-enriched, C_8-GluCer or C_8-GalCer enriched nanoliposomes. Nucleus was stained with Hoechst (*blue*). Doxorubicin is fluorescent by itself (*red*). At least three independent experiments were performed.

GalCer, but not C_8-LacCer appeared promising and displayed similar drug uptake enhancing properties as C_8-GluCer. Drug uptake enhancement by SCS-DoxNL significantly increased *in vitro* antitumor activity towards various human tumor cell lines. This effect was observed to a much lesser extent in normal endothelial cells and fibroblasts, demonstrating an important preference of this drug delivery process for tumor cells. Finally, we were able to demonstrate that enhanced Dox delivery by SCS-Dox-NL was not related to uptake of the nanoliposomes as such by the tumor cells, but was preceded by a rapid and apparently critical transfer of the SCS from the nanoliposomal bilayer to the cell membrane. A similar transfer process was proposed previously by Zolnik and co-workers for the apoptosis-inducing N-hexanoyl-d-erythrosphingosine (C_6-ceramide) (31). In the present study we demonstrated that the C_8-GluCer or C_8-GalCer upon their transfer to the tumor cell membrane do not affect cell survival in the absence of Dox, but are able to potentiate Dox cytotoxicity.

Optimal loading of Dox (> 90% encapsulation efficiency) in DoxNL enriched with 10 mol% C_8-GluCer or C_8-GalCer was obtained at a Dox:PL initial mass ratio of 0.1:1 resulting in homogeneous particles (pdi<0.1) with a size between 80 and 100 nm, which is considered ideal for efficient

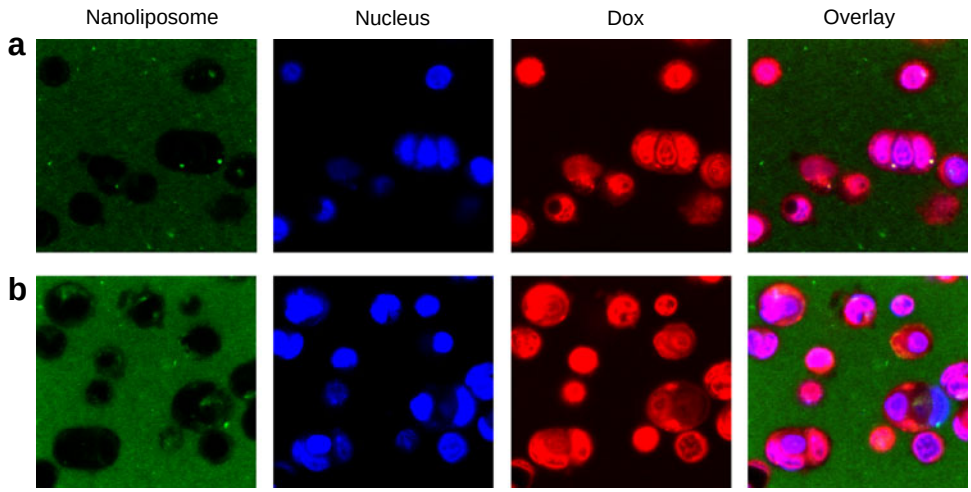

Fig. 7 Intracellular-localization of NBD-PE-labeled liposomes (*green*) and Dox (*red*) in MCF7 breast carcinoma cell line by confocal microscopy. Treatment was added (10 μM Dox) in the form of C_8-GluCer-DoxNL (**a**) or C_8-GalCer-DoxNL (**b**) and after 4 h of incubation at 37°C, nuclear (*blue*) and cytoplasmatic drug uptake were analyzed.

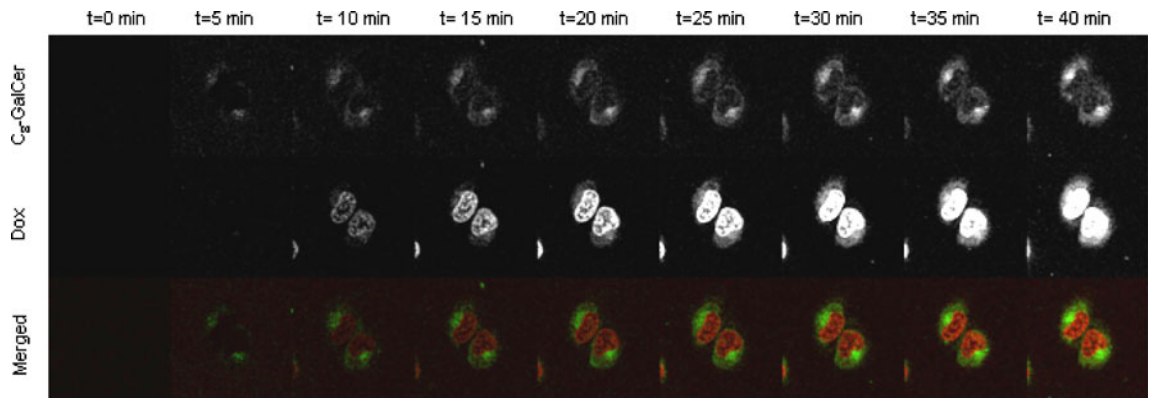

Fig. 8 Localization of SCS and Dox in the plasma membrane by confocal microscopy. Directly after starting BLM melanoma cell treatment, with 5 μM NBD labeled-SCS liposomal Dox, the green fluorescent labelled-C_8-GalCer and fluorescent Dox were followed in time. The SCS accumulates in the plasma membrane after which Dox accumulation in the nucleus takes place rapidly.

extravasation through leaky tumor vasculature (1,32). For SCS-DoxNL higher Dox:PL ratios caused somewhat less efficient drug loading, but did not affect drug efficacy towards BLM, melanoma and MCF7 breast carcinoma cell lines (Fig. 1a). This result suggests that the quantity of SCS used at the highest Dox:PL ratio of 0.25:1 was sufficient to induce maximal enhancement of drug uptake. This is in accordance with Veldman *et al.* who demonstrated that uptake of Dox, added to cells in free form, reached saturation upon treating these cells with increasing concentrations of C_6-sphingomyelin (6). Moreover, the higher quantity of SCS, in enriched liposomal formulations with lower Dox:PL mass ratios did not induce additional toxicity by the SCS. This correlates well with the finding that cytotoxicity is related to doxorubicin treatment and not to the SCS.

Formulation of C_8-LacCer in Dox-NL was unsuccessful. Despite the fact that C_8-LacCer enriched-NL could be prepared, Dox loading of these NL resulted in strong aggregation and low loading efficiency. Likely, the more complex sugar moiety of C_8-LacCer in comparison to C_8-GluCer or C_8-GalCer (Fig. 2) interfered with the liposomal membrane preventing a stable transmembrane ammonium sulfate gradient.

Whereas density of C_8-GalCer did not affect DoxNL size, pdi and Dox loading, *in vitro* drug efficacy was improved only for the 10 and 15 mol% enriched formulations in comparison to standard DoxNL. Since 10 mol% C_8-GalCer-DoxNL were equally effective as those with 15 mol%, we concluded that the former loaded at an initial Dox:PL mass ratio of 0.1:1 represented the optimal C_8-GalCer-DoxNL formulation. With a 10 mol% SCS-density and a 0.1:1 D:PL (w/w) loading ratio this optimal C_8-GalCer-DoxNL has similar characteristics as the optimal C_8-GluCer-DoxNL (8).

Stability studies under storage or cell culture conditions demonstrated both SCS-DoxNL formulations provided high stability and did not reveal significant differences between C_8-GluCer or C_8-GalCer enriched and standard DoxNL. Cryo-TEM elucidated a typical Dox precipitate inside all DoxNL (28) with a more prominent rod-shaped morphology for SCS-Dox-NL than DoxNL. Apparently the presence of SCS in the bilayer of DoxNL is responsible for the change in shape of the nanoparticles during Dox-loading, as SCS-liposomes before loading were round-shaped and after loading all rod-shaped particles did contain a clear Dox precipitate. Liposomal bilayers, when enriched with SCS, seemingly are more flexible or deformable. It remains speculative whether this enhanced flexibility of enriched liposomal bilayers contributes to the improved intracellular Dox delivery.

Both C_8-GluCer-DoxNL and C_8-GalCer-DoxNL significantly increased cytotoxicity in comparison to standard DoxNL and clinically applied DoxNL (Doxil/Caelyx) in all tumor cell lines tested. Stable Dox entrapment in Doxil is known to reduce toxic side effects related to free Dox. However, this high stability in combination with the low tumor cell membrane permeability for DoxNL strongly limits drug delivery and efficacy (22,23,33). It is at this point that drug delivery is improved when using SCS-DoxNL. Enrichment of DoxNL with C_8-GluCer or C_8-GalCer did not affect Dox release for up to 24 h in cell culture medium containing 10% of serum (Table II and Supplementary Material Figure S1), but was in a similar period able to improve *in vitro* drug efficacy, due to SCS potential as drug uptake enhancer. Remarkably, the *in vitro* cytotoxic effect of SCS-DoxNL was much less pronounced on endothelial cells and fibroblasts demonstrating a cell-type dependency and specificity of the SCS-drug delivery process in favor of tumor cells. In addition, this finding holds promise that SCS-DoxNL during circulation will not readily affect the normal endothelial lining of healthy blood vessels. Upon accumulation at the tumor site, SCS can act as a tumor cell membrane selective drug permeabilizer. In this context, similar results using SCS and Dox administered in free form, were reported by Veldman *et al.* with cultured rat cardiac myoblasts

(6). For yet unknown reasons, non-tumor cells are not highly susceptible towards the sphingolipid analogue mediated drug uptake enhancement, when compared to tumor cells.

The increased *in vitro* efficacy of SCS-DoxNL coincided with an increased and rapid intracellular drug delivery in different tumor cell lines as demonstrated by fluorescence microscopy and flow cytometry. Already within 1 h notable differences in cellular Dox fluorescence were measured between SCS-enriched and non-enriched DoxNL, in favor of the former. These differences appeared maximal after 4 h of incubation reaching up to 5-8-fold more Dox delivered using SCS-DoxNL and remained high until 24 h. In these drug uptake studies some variation between the sensitivity of various tumor cell lines towards SCS- DoxNL was observed. Dox uptake after incubation for 4 h with C_8-GluCer-DoxNL was higher in BLM melanoma than after C_8-GalCer-DoxNL. This difference was not observed with MCF7 breast and ASPC1 pancreatic carcinoma. These observations were confirmed by living cell fluorescence microscopy and suggest a difference in the potential of C_8-GluCer *versus* C_8-GalCer as drug uptake enhancers and that even among tumor cells certain cell specificity for each distinct SCS exists. Future studies will investigate whether differences in cell membrane lipid composition can explain the differences in SCS-mediated drug uptake in normal and tumor cells. An important question is how Dox is transported from the liposomes into the cell. Seynhaeve *et al.* concluded that, in addition to passive release, DoxNL may be taken up completely by tumor cells upon long-term incubations, followed by intracellular degradation, after which released Dox enters the nucleus (22). Others suggested that liposomes can be degraded in the interstitial space followed by uptake of the released drug by tumor cells (4,5,34–36). Our living cell confocal microscopy studies using SCS-DoxNL with a fluorescent bilayer marker, showed virtually no internalization of the nanoliposomal carrier by MCF7, ASPC1 or BLM cell lines during 4 h of incubation, whereas at the same time high levels of Dox where detected intracellularly in the nucleus and to a lesser extent in the cytoplasm. Therefore intracellular Dox delivery using SCS-NL is not dependent on internalization of the nanocarrier as such. By contrast, transfer of the SCS from the nanoliposomal bilayer to the tumor cell membrane was demonstrated to occur rapidly and to precede Dox influx. Together these data demonstrate that the selective transfer of the SCS to the tumor cell membrane promotes Dox internalization. Transfer of liposomal bilayer constituents to tumor cell membranes has been described previously for a lipophilic prodrug of 5-fluorodeoxyuridine and the anti-angiogenic drug fumagillin (37–39).

It remains to be seen whether the SCS transfer also enhances drug release from the liposomes. The transfer of SCS from the rod-shaped liposomal bilayer to the cell membrane when in close proximity may well be responsible for a locally enhanced release of Dox from the particles in which the SCS stabilized rod-like shape is deformed causing local content release at the sites of SCS transfer. The released content is then taken up more rapidly due to SCS induced permeability of the cell membrane. Pinnaduwage and Huang referred to a similar delivery process by liposomes that upon direct contact with a membrane-bound antigen, rapidly and spontaneously destabilize, releasing entrapped contents (40).

CONCLUSION

The findings presented here identified, C_8-GluCer and C_8-GalCer, as specific SCS to improve the therapeutic potential of nanoliposomal Dox by selectively enhancing cellular membrane permeability of tumor cells to Dox upon their transfer to the cell membrane. Optimized formulations of SCS-DoxNL were developed, which will now undergo *in vivo* evaluation to investigate if they are able to overcome the current issue of limited Dox bioavailability related to DoxNL.

ACKNOWLEDGMENTS AND DISCLOSURES

This work was financed by the Dutch Cancer Society.

REFERENCES

1. Gabizon A, Shmeeda H, Barenholz Y. Pharmacokinetics of pegylated liposomal dox: review of animal and human studies. Clin Pharmacokinet. 2003;42(5):419–36.
2. Koning GA, Krijger GC. Targeted multifunctional lipid based nanocarriers for image guided drug delivery. Anti Cancer Agents Med Chem. 2007;7(4):425–40.
3. Maeda H, Wu J, Sawa T, Matsumura Y, Hori K. Tumor vascular permeability and the EPR effect in macromolecular therapeutics: a review. J Contr Release. 2000;65(1–2):271–84.
4. Mayer D, Nayar R, Thies RL, Boman NL, Cullis PR, Bally MB. Identification of vesicle properties that enhance the antitumor activity of liposomal vincristine against murine L1210 leukemia. Cancer Chemother Pharmacol. 1993;33(1):17–24.
5. Mayer LD, Bally MB, Cullis PR, Wilson SL, Emerman JT. Comparison of free and liposome encapsulated Dox tumor drug uptake and antitumor efficacy in the SC115 murine mammary tumor. Cancer Lett. 1999;53(2–3):183–90.
6. Veldman RJ, Zerp S, van Blitterswijk WJ, Verheij M. N-hexanoyl-sphingomyelin potentiates *in vitro* Dox cytotoxicity by enhancing its cellular influx. Br J Cancer. 2004;90(4):917–25.
7. Veldman RJ, Koning GA, van Hell A, Zerp S, Vink SR, Storm G, *et al.* Coformulated N-Octanoyl-glucosylceramide improves cellular delivery and cytotoxicity of liposomal Dox. J Pharmacol Exp Ther. 2005;315(2):704–10.
8. van Lummel M, van Blitterswijk WJ, Vink SR, Veldman RJ, van der Valk MA, Schipper D, *et al.* Enriching lipid nanovesicles with short-chain glucosylceramide improves Dox delivery and efficacy in solid tumors. FASEB J. 2011;25(10):280–9.

9. Jacobson K, Mouritsen OG, Anderson RG. Lipid rafts: at a crossroad between cell biology and physics. Nat Cell Biol. 2007;9(1):7–14.
10. Anderson RG. The caveolae membrane system. Annu Rev Biochem. 1998;67:199–225.
11. Masserini M, Ravasi D. Role of sphingolipids in the biogenesis of membrane domains. Biochim Biophys Acta. 2001;1532(3):149–61.
12. Siskind LJ, Colombini M. Sphingosine forms channels in membranes that differ greatly from those by ceramide. J Bioenerg Biomembr. 2005;37(4):227–36.
13. Bodley A, Liu LF, Israel M, Seshadri R, Koseki Y, Giuliani FC, *et al.* DNA Topoisomerase II-mediated interaction of Dox and daunorubicin congeners with DNA. Cancer Res. 1989;49(21):5969–78.
14. Gewirtz DA. A critical evaluation of the mechanisms of action proposed for the antitumor effects of the anthracycline antibiotics adriamycin and daunorubicin. Biochem Pharmacol. 1999;57(7):727–41.
15. Rahman AM, Yusuf SW, Ewer MS. Anthracycline-induced cardiotoxicity and the cardiac-sparing effect of liposomal formulation. Int J Nanomedicine. 2007;2(4):567–83.
16. O'Brien ME, Wigler N, Inbar M, Rosso R, Grischke E, Santoro A, *et al.* CAELYX Breast Cancer Study Group, Reduced cardiotoxicity and comparable efficacy in a phase III trial of pegylated liposomal Dox HCl (CAELYX/DoxilÂ®) *versus* conventional Dox for first-line treatment of metastatic breast cancer. Ann Oncol. 2004;15(3):440–9.
17. Torchilin VP, Omelyanenko VG, Papisov MI, Bogdanov Jr AA, Trubetskoy VS, Herron JN, *et al.* Poly (ethylene glycol) on the liposome surface: on the mechanism of polymer-coated liposome longevity. Biochim Biophys Acta. 1994;1195(1):11–20.
18. Northfelt DW, Dezube BJ, Thommes JA, Miller BJ, Fischl MA, Friedman-Kien A, *et al.* Pegylated-liposomal Dox *versus* Dox, bleomycin, and vincristine in the treatment of AIDS-related Kaposi's sarcoma: results of a randomized phase III clinical trial. J Clin Oncol. 1998;16(7):2445–51.
19. Tejada-Berges T, Granai CO, Gordinier M, Gajewski W. Caelyx/Doxil for the treatment of metastatic ovarian and breast cancer. Expert Rev Anticancer Ther. 2002;2(2):143–50.
20. Hussein MA, Anderson KC. Role of liposomal anthracyclines in the treatment of multiple myeloma. Semin Oncol. 2006;31 (6 Suppl 13):147–60.
21. Alberts DS, Liu PY, Wilczynski SP, Clouser MC, Lopez AM, Michelin DP, *et al.* Randomized trial of pegylated liposomal Dox (PLD) plus carboplatin *versus* carboplatin in platinum-sensitive (PS) patients with recurrent epithelial ovarian or peritoneal carcinoma after failure of initial platinum-based chemotherapy (Southwest Oncology Group Protocol S0200). Gynecol Oncol. 2008;108(1):90–4.
22. Seynhaeve AL, Hoving S, Schipper D, Vermeulen CE, Wiel-Ambagtsheer G, van Tiel ST, *et al.* Tumor necrosis factor a mediates homogeneous distribution of liposomes in murine melanoma that contributes to a better tumor response. Cancer Res. 2007;67(19):9455–62.
23. Laginha KM, Verwoert S, Charrois GJ, Allen TM. Determination of doxorubicin levels in whole tumor and tumor nuclei in murine breast cancer tumors. Clin Cancer Res. 2005;11(19 Pt 1):6944–9.
24. Judson I, Radford JA, Harris M, Blay JY, van Hoesel Q, le Cesne A, *et al.* Randomised phase II trial of pegylated liposomal doxorubicin (DOXIL/CAELYX) *versus* doxorubicin in the treatment of advanced or metastatic soft tissue sarcoma: a study by the EORTC Soft Tissue and Bone Sarcoma Group. Eur J Cancer. 2001;37(7):870–7.
25. Haran G, Cohen R, Bar LK, Barenholz Y. Transmembrane ammonium sulfate gradients in liposomes produce efficient and stable entrapment of amphipathic weak bases. Biochim Biophys Acta. 1993;1151(2):201–15.
26. Rouser G, Fkeischer S, Yamamoto A. Two dimensional thin layer chromatographic separation of polar lipids and determination of phospholipids by phosphorus analysis of spots. Lipids. 1970;5 (5):494–6.
27. Li X, Hirsh DJ, Cabral-Lilly D, Zirkel A, Gruner SM, Janoff AS, *et al.* Dox physical state in solution and inside liposomes loaded *via* a pH gradient. Biochim Biophys Acta. 1998;1415(1):23–40.
28. Maurer-Spurej E, Wong KF, Maurer N, Fenske DB, Cullis PR. Factors influencing uptake and retention of amino-containing drugs in large unilamellar vesicles exhibiting transmembrane pH gradients. Biochim Biophys Acta. 1999;1416(1–2):1–10.
29. Jaffe EA, Becker CG, Minick CR. Culture of human endothelial cells derived from umbilical veins. Identification by morphologic and immunologic criteria. J Clin Invest. 1973;52(11):2745–56.
30. Skehan P, Storeng R, Scudiero D, Monks A, McMahon J, Vistica D, *et al.* New colorimetric cytotoxicity assay for anticancer-drug screening. J Natl Cancer Inst. 1990;82(13):1107–12.
31. Zolnik BS, Stern ST, Kaiser JM, Heakal Y, Clogston JD, Kester M, *et al.* Rapid distribution of liposomal short chain ceramide *in vitro* and *in vivo*. Drug Metab Dispos. 2008;36(8):1709–15.
32. Charrois GJ, Allen TM. Rate of biodistribution of STEALTH liposomes to tumor and skin: influence of liposome diameter and implications for toxicity and therapeutic activity. Biochim Biophys Acta. 2003;1609(1):102–8.
33. Bandekar A, Karve S, Chang M, Mu Q, Rotolo J, Sofou S. Antitumor efficacy following the intracellular and interstitial release of liposomal doxorubicin. Biomaterials. 2012;33:4345–52.
34. Forssen EA, Coulter DM, Proffitt RT. Selective *in vivo* localization of daunorubicin small unilamellar vesicles in solid tumors. Cancer Res. 1992;52(12):3255–61.
35. Gabizon AA. Selective tumor localization and improved therapeutic index of anthracyclines encapsulated in long-circulating liposomes. Cancer Res. 1992;52(4):891–6.
36. Perez-Soler R, Ling YH, Zou Y, Priebe W. Cellular pharmacology of the partially non-cross-resistant anthracycline annamycin entrapped in liposomes in KB and KB-V1 cells. Cancer Chemother Pharmacol. 1994;34(2):109–18.
37. Koning GA, Morselt HW, Velinova MJ, Gorter A, Allen TM, Zalipsky S, *Et al.*,Selective transfer of a lipophilic prodrug of 5-fluorodeoxyuridine from immunoliposomes to colon cancer cells. Biochim Biophys Acta. 1999;1420(1–2):153–67.
38. Koning GA, Gorter A, Scherphof GL, Kamps JA. Antiproliferative effect of immunoliposomes containing 5-fluorodeoxyuridine-dipalmitate on colon cancer cells. Br J Cancer. 1999;80(11):1718–25.
39. Cyrus T, Winter PM, Caruthers SD, Wickline SA, Lanza GM. Magnetic resonance nanoparticles for cardiovascular molecular imaging and therapy. Expert Rev Cardiovasc Ther. 2005;3(4):705–15.
40. Pinnaduwage P, Huang L. Stable Target-Sensitive immunoliposomes. Biochemistry. 1992;31:2850–5.